

Cite this article as: Su Guang, Zhang Aimin, Wei Jiahong. Atomic Mechanism of α -Al Heterogeneously Nucleating on AlB_2 in Al-Si Alloy[J]. Rare Metal Materials and Engineering, 2021, 50(06): 1964-1970.

ARTICLE

Atomic Mechanism of α -Al Heterogeneously Nucleating on AlB_2 in Al-Si Alloy

Su Guang¹, Zhang Aimin¹, Wei Jiahong²

¹Department of Material Science and Engineering, Henan Institute of Technology, Xinxiang 453000, China; ²Department of Electrical Engineering and Automation, Henan Institute of Technology, Xinxiang 453000, China

Abstract: The valence electron structure and cohesive energy of α -Al, AlB_2 and $(\text{Al-Si})\text{B}_2$ crystals were calculated using the empirical electron theory (EET) of solids and molecules. The calculated results indicate that Al-Al atomic layer on outermost surface of AlB_2 is relatively unstable and the cohesive energy of both α -Al and AlB_2 decrease with increase of Si content in Al-Si melt. According to the calculated results, a novel atomic mechanism of α -Al heterogeneously nucleating on AlB_2 in Al-Si alloy is explored. After adding additional Si, a certain amount of Si atoms enter into AlB_2 , which results in formation of a stable Al-Si binary atomic structure layer on AlB_2 surface and finally improves the stability of AlB_2 . This two-dimensional Al-Si atomic layer plays an important transition role in the subsequent heterogeneous nucleation process, which is responsible for the atomic mechanism of nucleation of α -Al attached to AlB_2 .

Key words: AlB_2 crystal structure; Al-Si alloy; heterogeneous nucleation; atomic mechanism; EET of solids and molecules

It is well known that, adding potent agent into aluminum alloy melt during solidification process will contribute to modifying as-cast microstructure and improving mechanical properties. Although Al-5Ti-1B master alloy is an excellent commercial refiner for most wrought aluminum alloys^[1-3], silicon element in foundry Al-Si alloy will severely deteriorate the refining efficiency of Al-5Ti-1B through reacting with Ti element and forming intermetallic, i.e. Ti_3Si_3 ^[4] or segregating in the TiAl_3 two-dimensional compound (2DC)^[5]. While for Al-Si alloy, the binary Al-B series master alloy without Ti element was developed as a more efficient refiner than Al-Ti-B with excessive Ti^[6-9]. However, despite the common consensus of Al-B series master alloy being able to refine the microstructure of Al-Si alloy, of which precise refining mechanism is still not clear up to now^[6-9].

In previous research^[10], the grain refining mechanism of Al-Si alloys with addition of B is simply attributed to the eutectic reaction between Al and B. However, this eutectic reaction mechanism cannot explain the fading phenomenon of Al-B refiner and the different refining performance for Al-Si, Al-

Mg, Al-Zn and Al-Cu alloys^[11]. According to the eutectic reaction mechanism, AlB_2 particles in Al-B master alloy should dissolve absolutely and exist in the form of B atom, from which it can be inferred that the grain size of α -Al is not supposed to coarse with increasing the inoculation time^[12]. However, Vinod Kumar's work^[13] shows that the completely dissolution of AlB_2 particles in Al-B alloy melt will last more than 60 min at 720 °C. In addition, Wang^[14] investigated the effects of morphology and size of AlB_2 particles in different Al-3B alloys on grain refinement of Al-7Si alloy, suggesting that the Al-B refiner with a larger size of AlB_2 particle has an obvious fading phenomenon. Besides, although with a perfect performance in refining Al-Si alloys, Al-B master alloy is experimentally confirmed to have different refining efficiencies in Al-Mg, Al-Zn and Al-Cu alloys^[11]. In a word, it seems that the experimental results mentioned above cannot all be interpreted by the eutectic reaction mechanism.

Because the integrated AlB_2 particles are already examined inside of α -Al, other mechanism of heterogeneous nucleation of α -Al is proposed for Al-Si alloy inoculated by Al-B refiner.

Received date: September 09, 2020

Foundation item: Training Program of Young Scholar in College and University of Henan Province (2017GGJS168); PHD Scientific Research Initial Foundation of Henan Institute of Technology (KQ1848)

Corresponding author: Zhang Aimin, Ph. D., Department of Material Science and Engineering, Henan Institute of Technology, Xinxiang 453000, P. R. China, E-mail: zhangaimin@hait.edu.cn

Copyright © 2021, Northwest Institute for Nonferrous Metal Research. Published by Science Press. All rights reserved.

However, it is noted that the unstable AlB_2 particles cannot work as an efficient heterogeneous substrate in purity Al melt^[6,15]. Although AlB_2 particles are not stable enough to be a potential nucleating substrate, addition of Si can decrease the melting point of purity Al melt and promote the formation and stability of AlB_2 in Al-Si melt before the crystallization of α -Al^[16,17]. The main point is why these AlB_2 particles become stable before crystallization of α -Al and what is the precise nucleation mechanism of AlB_2 particle for α -Al in Al-Si alloy.

It is well documented that the interfacial structure of solid/liquid (S/L), especially the atomic structure and composition of S/L interface, is the essential factor that controls the efficiency and potency of heterogeneous particle^[18]. Han^[19] calculated the interfacial energy of α -Al(111)/ AlB_2 (0001) using density functional theory (DFT), and the results show that the interfacial energy of α -Al(111)/ AlB_2 (0001) is greater than that between primary Al phase and aluminum melts, which indicates that pure α -Al might not be refined by AlB_2 . However, Si elements were not involved in their calculation model. Chen^[20] inferred that Si might react with AlB_2 to form a layer of SiB_6 at the interface of α -Al/ AlB_2 , which may reduce the crystallographic mismatch and promote the grain refining efficiency of AlB_2 . However, it is not SiB_6 but Si nanoparticles were examined nearby the interface of α -Al/ AlB_2 .

In this work, we calculated the valence electron structure of two kinds of Al and AlB_2 crystals using empirical electron theory (EET) of solids and molecules. Based on the calculated results, the stabilizing mechanism of AlB_2 and the accurate atomic mechanism for grain refining of Al-Si alloy with B element were elucidated. Some fresh insights about the heterogeneous nucleation of α -Al on AlB_2 were proposed.

1 Calculation Method

The empirical electron theory (EET) of solids and molecules was employed in this work. Since it was established by Yu Ruihuang in 1978^[21], the EET have been developed considerably, especially in the improvement of multi-solutions and calculation accuracy^[21-23], which has been widely applied in material fields^[24-29]. In EET, a multi-calculational model can be easily established without considering the special position of doping elements^[26,27], and the average variation of bond energy and cohesive energy can be predicted. In the present study, the electron structure of α -Al containing Si, AlB_2 and AlB_2 doped with Si was studied through EET calculations.

1.1 Calculations of valence electron structure (VES) of α -Al and AlB_2

In EET, it is considered that the VES generally consists of the covalent bonds formed by atoms, the electron distribution on covalent bonds, and the atomic states. The analysis models for VES used in this study are presented in Fig. 1, i.e., initial pure Al (Fig. 1a) and α -Al containing different contents of Si atoms (Fig. 1b), initial pure AlB_2 (Fig. 1c) and AlB_2 doped with different contents of Si atoms (Fig. 1d). According to the supposed calculation models given in Ref. [26, 27], it is assumed that the doped Si atom and Al atom in α -Al and AlB_2 make up a kind of mixing atom, which including $(1-x)\text{Al}$ atoms and $x\text{Si}$ atoms ($x=1, 2, 3\cdots 9, 10$, at%). These mixing atoms still locate at the original positions of Al atoms in Al and AlB_2 surface, as illustrated in Fig. 1b and Fig. 1d.

The calculation process and results of Al can refer to Ref. [23], and the calculation process of α -Al containing different content of Si is the same as that of Al. The detail calculation steps of AlB_2 and $(\text{Al}-x\text{Si})\text{B}_2$ are present in the follows.

The lattice constants of AlB_2 , with a non-close packed hexagonal structure, are $a=b=0.3016$ nm and $c=0.3268$ nm. There are one aluminum atom and two boron atoms in each unit cell, and these atomic positions are shown in Table 1.

We used the bond length difference (BLD) method^[29,30] and the advanced self-consistent bond length difference (SCBLD)

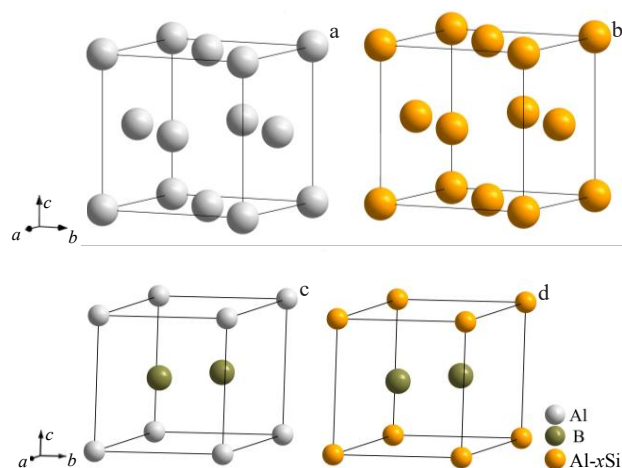


Fig.1 Analysis models of VES for fcc-structured Al (a), Al-xSi (b), hcp-structured AlB_2 (c), and AlB_2 doped with $x\text{Si}$ (d) structure units

Table 1 Atom positions in AlB_2 unit cell

Structure type AlB_2	Pearson symbol	Space group	Space group No.
Multiplicity	Coordinates: (0,0,0; 1/3,2/3,1/2; 2/3,1/3,1/2)		
Wyckoff letter	x	y	z
Al, 6c, 3m	0	0	0
B1, 2d, $\bar{6}/m2$	1/3	2/3	1/2
B2, 2d, $\bar{6}/m2$	2/3	1/3	1/2

method^[22,23] in EET to calculate the VES parameters of AlB₂ and (Al-xSi)B₂, respectively. The detail calculation steps for VES of two kinds of AlB₂ crystal are given in the follows.

In EET, Al and B atoms have the same head and tail states, given as Table 2.

On the basis of the hybridization states of Al and B, we can obtain $l=2, m=1, n=0, \tau=0; l'=1, m'=2, n'=0, \tau'=1$; for Al element, $R(1)_h=0.0763$ nm, $R(1)_i=0.0763$ nm; for B element, $R(1)_h=0.11900$ nm, $R(1)_i=0.11900$ nm.

The attendant hybridization results of Al and B elements can be obtained by substituting the above parameters into k -formula^[22], which are listed in Table 3.

In AlB₂ structure unit, nine kinds of covalent bonds are considered. Their covalent bond name (CBN, B_a^{B-B}), experimental bond length (EBL, B_{na}^{u-v}), equivalent bond number (EBN, I_a) are given in the follows. Here, u and v represent the atoms that form covalent bonds. The calculation formula of EBN is $I_a=I_M \cdot I_S \cdot I_K$, in which the meaning of I_M, I_S and I_K can be found in Ref. [30].

$$\begin{aligned} B_{n1}^{B-B}, D_{n1}^{B-B} &= 0.17411 \text{ nm}, I_1 = 2/3 \times 3 \times 1 = 2 \\ B_{n2}^{B-B}, D_{n2}^{B-B} &= 0.30160 \text{ nm}, I_2 = 2/3 \times 6 \times 1 = 4 \\ B_{n3}^{B-B}, D_{n3}^{B-B} &= 0.32680 \text{ nm}, I_3 = 2/3 \times 2 \times 1 = 1.33333 \\ B_{n4}^{B-B}, D_{n4}^{B-B} &= 0.37029 \text{ nm}, I_4 = 2/3 \times 6 \times 1 = 4 \\ B_{n5}^{B-B}, D_{n5}^{B-B} &= 0.34825 \text{ nm}, I_5 = 2/3 \times 3 \times 1 = 2 \\ B_{n6}^{Al-Al}, D_{n6}^{Al-Al} &= 0.32680 \text{ nm}, I_6 = 1/3 \times 2 \times 1 = 0.66667 \\ B_{n7}^{Al-Al}, D_{n7}^{Al-Al} &= 0.30160 \text{ nm}, I_7 = 1/3 \times 6 \times 1 = 2 \\ B_{n8}^{Al-B}, D_{n8}^{Al-B} &= 0.38468 \text{ nm}, I_8 = 1/3 \times 12 \times 2 = 8 \\ B_{n9}^{Al-B}, D_{n9}^{Al-B} &= 0.23880 \text{ nm}, I_9 = 1/3 \times 12 \times 2 = 8 \end{aligned}$$

Firstly, we obtained the optimal lattice constants and β parameter for AlB₂ structure using software of SCBLD, and the results are $a=b=0.30179$ nm, $c=0.32681$ nm, and $\beta=0.05264$. Then the VES parameters of AlB₂ structure unit were obtained by substituting the optimal lattice constants and β parameter into the equations of BLD method, and the

calculated results are shown in Table 4.

Although with the same analysis procedures of SCBLD and BLD for two kinds of AlB₂, i.e. AlB₂ structure units and AlB₂ doped with Si structure unit, the atom character parameters are also distinct. In AlB₂ doped with Si structure unit, Al atoms are replaced by the mixed atoms of Al and Si atoms. Therefore, the characteristic parameters of the mixed atoms are the weighted average with respect to that of Al and Si atoms, which are gained from Eq. (1).

$$\left. \begin{aligned} R_x(1) &= (1-x)R_{Al}(1) + xR_{Si}(1) \\ n_c^x &= (1-x)n_c^{Al} + xn_c^{Si} \\ n_m^x &= (1-x)n_m^{Al} + xn_m^{Si} \\ n_d^x &= (1-x)n_d^{Al} + xn_d^{Si} \\ f_x &= (1-x)f_{Al} + xf_{Si} \\ b_x &= (1-x)b_{Al} + xb_{Si} \end{aligned} \right\} \quad (1)$$

where x represents the atom percentage, and the meaning of the characteristic parameters of an atom, such as the covalent electron number n_c , the lattice electron number n_l , the magnetic electron number n_m , the dumb pair electron number n_d , the bond-forming ability f , and the shielding factor b is referred to Ref.[29].

Based on the calculated results of above parameters and the experimental lattice constants, the VES parameters of AlB₂ doped with Si structure units are obtained by calculation software of SCBLD and BLD methods, and part of the corresponding calculated results are presented in Table 5. Using the same method, we also calculated the VES parameters of Al doped Si structure units.

1.2 Calculation of cohesive energy of α -Al and AlB₂ doped with Si

The covalent bond energies and the cohesive energy of α -Al and AlB₂ crystals were calculated by the calculated VES parameters. The corresponding system of equations for bond energies (E'_a) and their statistical values in the structure unit are shown in the follows.

Table 2 Head and tail states of Al and B atoms

State	Orbit	s	p
Head	s ² p ¹	⬇	●○○
Tail	s ¹ p ²	●	●●○

Table 3 Hybridization results of Al and B element

σ	1	2	3	4	5	6
$C_{h\sigma}$	1	0.9835	0.9133	0.2352	0.0515	0
$C_{i\sigma}$	0	0.0165	0.0867	0.7648	0.9485	1
$n_{T\sigma}$	3	3	3	3	33	3
$n_{i\sigma}$	2	1.9670	1.8266	0.4704	0.1030	0
$n_{c\sigma}$	1	1.0330	1.1734	2.5296	2.8970	3
$R'_a(1)/\text{nm}$ of B	0.07980	0.07980	0.07980	0.07980	0.07980	0.07980
$R'_a(1)/\text{nm}$ of Al	0.11900	0.11900	0.11900	0.11900	0.11900	0.11900

Table 4 Calculated results of VES parameters, bond energies E'_a and cohesive energies ($E_c=386.3652$ kJ/mol) of AlB₂

CBN	EBN	EBL/nm	n'_a	$E'_a/\text{kJ}\cdot\text{mol}^{-1}$
B_{n1}^{B-B}	2	0.174243	0.5321689	93.52962
B_{n2}^{B-B}	4	0.301799	2.008459×10^{-3}	0.2036029
B_{n3}^{B-B}	1.33333	0.32680	6.728566×10^{-4}	6.29851×10^{-2}
B_{n4}^{B-B}	4	0.370349	1.001418×10^{-4}	8.27070×10^{-3}
B_{n5}^{B-B}	2	0.348485	2.605976×10^{-4}	2.28745×10^{-2}
B_{n6}^{Al-Al}	0.66667	0.32680	2.076272×10^{-2}	1.796062
B_{n7}^{Al-Al}	2	0.30180	6.197375×10^{-2}	5.806401
B_{n8}^{Al-B}	8	0.384894	2.944396×10^{-4}	2.25996×10^{-2}
B_{n9}^{Al-B}	8	0.238872	0.1749686	21.66041

Table 5 Selective calculated results of bond energies E'_a and cohesive energies for AlB_2 doped with different contents of Si ($kJ \cdot mol^{-1}$)

Calculated value	CBN	Si content/at%					
		1	2	3	4	5	6
E'_a	B_{n1}^{B-B}	93.77351	93.1377	92.79983	92.73057	92.91596	92.35792
	B_{n2}^{B-B}	0.204922	0.203577	0.202860	0.202710	0.203097	0.201916
	B_{n3}^{B-B}	0.062800	6.239E-2	6.217E-2	6.212E-2	6.224E-2	6.188E-2
	B_{n4}^{B-B}	8.267E-3	8.214E-3	8.185E-3	8.179E-3	8.194E-3	8.147E-3
	B_{n5}^{B-B}	2.305E-2	2.290E-2	2.282E-2	2.281E-2	2.285E-2	2.272E-2
	B_{n6}^{Al-Al}	1.783691	1.756332	1.73779	1.727081	1.723764	1.697285
	B_{n7}^{Al-Al}	5.820829	5.731423	5.670848	5.635888	5.625101	5.538596
	B_{n8}^{Al-B}	0.022707	0.022464	0.022308	0.022232	0.02223	0.02200
	B_{n9}^{Al-B}	21.63667	21.40142	21.25187	21.179	21.17862	20.95737
\bar{E}_C		386.6526	384.0399	382.4914	381.8942	382.1962	379.7975

$$\left. \begin{aligned}
 E'_a &= \sum_{i=1}^{\sigma_N} E_{ai} \cdot c_i \\
 E_{ai} &= b \sum \frac{I_a n_a}{D_{na}} f \\
 b &= \frac{31.395}{n - 0.36\delta} \\
 f &= \sqrt{\alpha_s} + \sqrt{3\beta_p} + g\sqrt{5\gamma_d}
 \end{aligned} \right\} (2)$$

where the meaning of calculation parameters can be found in Ref. [23].

Furthermore, we calculated the cohesive energy \bar{E}_C and its statistical values of structure unit according to the system of Eq.(3).

$$\left. \begin{aligned}
 \bar{E}_C &= b \left\{ \sum_a \frac{I_a n_a}{D_{na}} f + \frac{n_f}{D} f' + km^{3d} - CW \right\} \\
 \bar{E}'_C &= \sum_{i=1}^{\sigma_N} \bar{E}_{Ci} \cdot c_i
 \end{aligned} \right\} (3)$$

where the meaning and solving of above calculation parameters can also be obtained in Ref. [23].

Using the BLD and SCBLD software, the bond energies and cohesive energy of α -Al, AlB_2 and $(Al-xSi)/B_2$ structure units were obtained, and the calculated results are also shown in Table 4 and Table 5 and Fig.3.

2 Results and Discussion

2.1 Surface stability of AlB_2 based on EET results

Based on the VES parameters and the bond energies of Al and AlB_2 , the distribution and structure of main bonds in the two cells are illustrated in Fig.2. Combined with the calculated results shown in Table 4 and Fig. 2a, the basic structure of AlB_2 can be regarded as a sandwich structure, i.e., one B-B layer with main strong B-B bonds (bond energy is about 93.53 kJ/mol) in the middle of two Al-Al layers which have extremely small Al-Al bond energy (about 5.63 kJ/mol). The binding of Al-Al layer and B-B layer entirely depends on Al-B bond, and the energy of Al-B bond is only about 21.66 kJ/mol, which implies that the interatomic force between Al atom and B atom is far smaller than that of B-B atom. That is to say, in

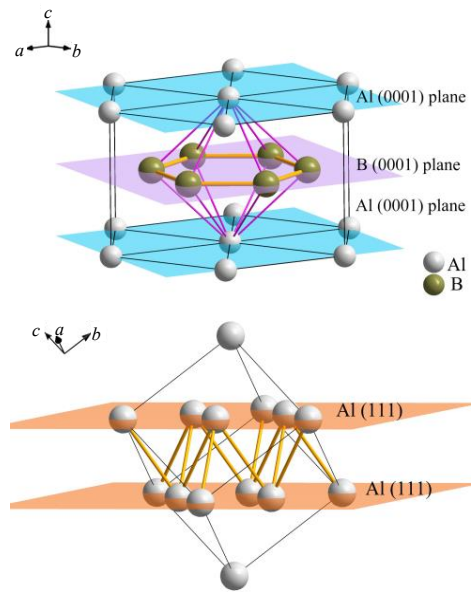


Fig.2 Diagram for distribution and structure of main bonds in AlB_2 (a) and Al (b) unite cells

the AlB_2 structure, B-B atomic layer plays the main role in the stability of the whole structure. For Al-Al layer, when it is inside of AlB_2 structure, Al-Al layer is sandwiched in the middle of B-B layer, which is not easy to decompose; when Al-Al layer is on the outermost surface of AlB_2 , it seems to decompose prior to B-B layer under certain temperature conditions. Additionally, the binding energy of Al-Al bond between (111) planes (Fig.2b) in Al crystal is also larger than that of Al-B bond and Al-Al bond on (0001) planes in AlB_2 . As a consequence, it is inferred that Al-Al atomic layer on the outermost surface of AlB_2 , which has lower Al-B bond energy and binding energy, may not be stable enough, especially under high-temperature pure aluminum melt conditions.

It is worth noting that the surface instability of AlB_2 is not only related to its own structure, but also closely related to its surface composition. Although the cohesive energy of AlB_2 is relatively larger than that of Al, it is still unable to form stable

AlB₂ prior to α -Al when the composition of B is lower than eutectic point according to the Al-B phase diagram. For the same reason, even under the condition of sufficient B content, the local B content on the final growing surface of AlB₂ must be very small compared with the Al content in melt, and the Al-B bond is weak relative to B-B bond, so the surface of AlB₂ terminated with Al atoms is probable to be unstable under certain conditions. Therefore, it is necessary to stabilize the Al-Al layer on AlB₂ surface to make it easy to combine and become stable enough.

2.2 Effect mechanism of Si on the nucleation undercooling of AlB₂

According to the above discussion, in order to make the Al-Al layer on the surface of AlB₂ form a stable structure in the deficiency of B, increasing the melt undercooling is one of the effective method. That is, adding additional alloy elements to impede the nucleation of matrix alloy, further reducing the freezing point of the α -Al, finally promoting the formation and stability of AlB₂, and then activate AlB₂ to become effective heterogeneous nucleus.

The addition of Si into Al melt will decrease the melting point and increase the nucleation undercooling. The effect of Si on the Al-Al bond energy and cohesive energy of Al is shown in Fig.3. It can be seen from Fig.3 that both the Al-Al bond energy and the cohesive energy of Al decrease with the increase of Si content. It indicates that the impeding effect of Si on the aggregation and nucleation of Al atoms is gradually enhanced in the liquid phase state, which is the main reason why the melting point of Al-Si alloy decreases with the increase of Si content.

However, without the addition of B, the increase of undercooling caused by Si does not completely transform into the nucleation power of α -Al. On contrary, α -Al grain becomes coarser when Si content is over a certain level, and the change of Al-Si alloy grain size as a function of Si content is shown in Fig.4. As can be seen from Fig.4, a few amounts of Si in Al-Si melt refine the grain of Al-Si alloy. While in the case of abundant Si (more than 4wt%) in Al melt, the grain of Al-Si alloy grows up with increasing the Si content^[17,20,31]. This

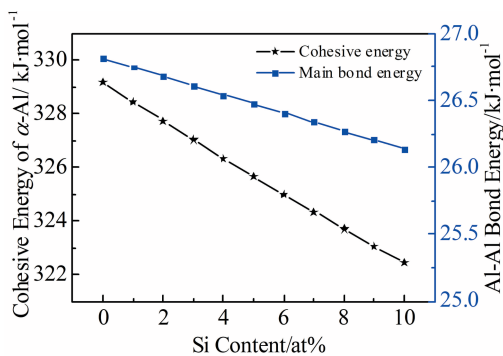


Fig.3 Variation of Al-Al bond energy and cohesive energy of α -Al doped with content of Si

phenomenon can be no longer explained by growth restriction factor (GRF) theory^[32]. It can also be seen from Fig.4 that with the presence of B, α -Al is refined when Si content is more than 4wt%, which indicates that AlB₂ is successfully activated under high undercooling of melt. It should be noted that when the undercooling degree of the melt is relatively low, i.e. when the content of Si is below 4wt%, α -Al can still not be refined, which indicates that AlB₂ is not stable enough.

2.3 Atomic mechanism of Si on the surface stability of AlB₂

The traditional criterion of heterogeneous nucleation is on the basis of crystallographic characteristic, i.e., atomic arrangement misfit between nucleating substrate and matrix, which is evidently not adequate to describe the mechanism of heterogeneous nucleation^[18,33,34]. From our previous study on the mechanism of α -Mg heterogeneously nucleating on Al₄C₃, it is considered that both the interfacial composition and the atomic arrangement misfit are necessary conditions required for heterogeneous nucleation^[35]. Therefore, besides the condition of satisfying lattice matching, other critical factor for the heterogeneous particles to be potent nucleus is that there is a stable surface with similar composition to the matrix.

In the case of α -Al nucleating on AlB₂, although both the crystal structure and the surface constituent of AlB₂ seem already satisfy the requirement for a promising nuclei of α -Al, the ultimate surface of AlB₂ is unstable in molten pure Al and Al with little Si. In order to analyze the effect mechanism of Si on the surface stability of AlB₂, the cohesive energies of AlB₂ with different Si contents were calculated. The variation of AlB₂ cohesive energy and the primary Al-B bond energy with Si content is illustrated in Fig.5. It can be seen from Fig.5 that the cohesive energy of AlB₂ and the Al-B bond energy both decrease with the increment of Si content inside of AlB₂. It is obvious that when the content of Si is more than 4at%, the decreasing trend is more significant, and it is particularly interesting that the value of inflection point roughly coincides with Fig.4. It is not difficult to understand that when the content of B is insufficient, the binding of AlB₂ becomes difficult. At this time, if the cohesive energy of AlB₂ is reduced, the binding and stability of Al-Al layer on the

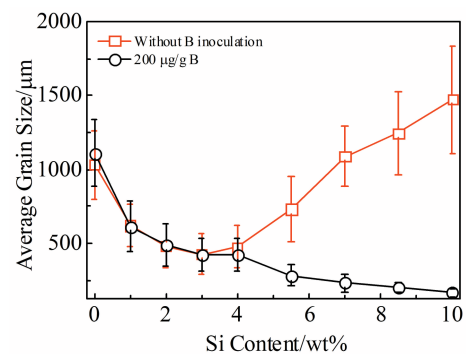


Fig.4 Variation of average grain size with Si content in Al-Si alloys with and without B (redrawn from Ref.[20])

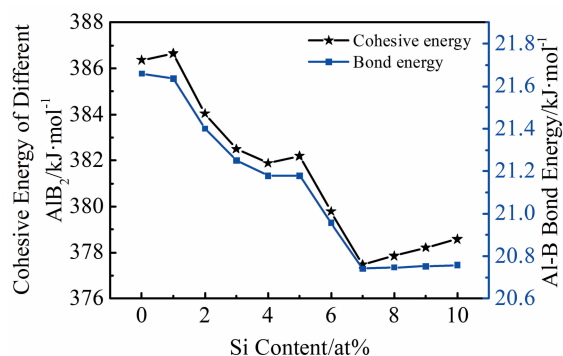


Fig.5 Variation of Al-B bond energy and cohesive energy of AlB_2 doped with different contents of Si

outermost plane of AlB_2 will be improved. Combined with the previous analysis, it is reasonable to infer that the decrease of cohesive energy of AlB_2 is beneficial to the formation of AlB_2 and the stability of Al-Al atomic layer on AlB_2 surface. As a result, the newly formed surface of AlB_2 , i.e. the two-dimensional Al-Si atomic layer, tends to be stable gradually with increasing the Si content, especially when the Si content is beyond about 4at%.

In addition, the formation sequence of AlB_2 is susceptible to Si concentration based on the calculated Al-Si-B phase diagram^[16], and the AlB_2 particles form easily when the Si content is beyond about 4at%. The simulated results of Al-7Si-0.2B using Thermo-Calc software package give the solidification path as: liquid $\rightarrow\text{AlB}_2$ +liquid $\rightarrow\text{AlB}_2$ +Al+liquid $\rightarrow\text{AlB}_2$ +Si+Al+liquid. Meanwhile, according to the Si-B binary phase diagram^[36], when the content of B is less than 3at%, B is dissolved in Si matrix and does not tend to form SiB_6 . However, when the Si content in Al-Si-B alloy exceeds 4at%, the B/Si value is lower than 3at%. Therefore, it is reasonable to infer that the influence of Si on AlB_2 is not achieved by changing the existing form of AlB_2 , but by changing its surface composition.

Based on the foregoing hypothesis and discussion, we proposed a novel atomic mechanism model to reveal the grain refining mechanism of Al-Si alloy refined with B element, as shown in Fig.6. Firstly, as shown in Fig.6a, the Al-Al layer on the outermost surface of AlB_2 in high temperature aluminum melt will dissolve prior to B-B layers. Then, some Al-Si atomic clusters in Al-Si liquid are preferentially adsorbed by B-B atomic layer for low formation energy of $(\text{Al}-x\% \text{Si})\text{B}_2$ structure and Al/Si-B bond (Fig.6b). Thus, the new stable Al-Al atomic plane containing Si content is formed, i.e. the two-dimensional Al-Si atomic layer, which eventually is supposed to be responsible for grain refining mechanism of Al-Si alloy inoculated with B element.

2.4 Precipitation reason of nano Si on AlB_2 surface

Normally, initial α -Al contains little Si compared with Al-Si alloy composition, and most Si can quickly and completely diffuse outside of α -Al with decreasing the temperature in subsequent solidification to form eutectic Si because of the

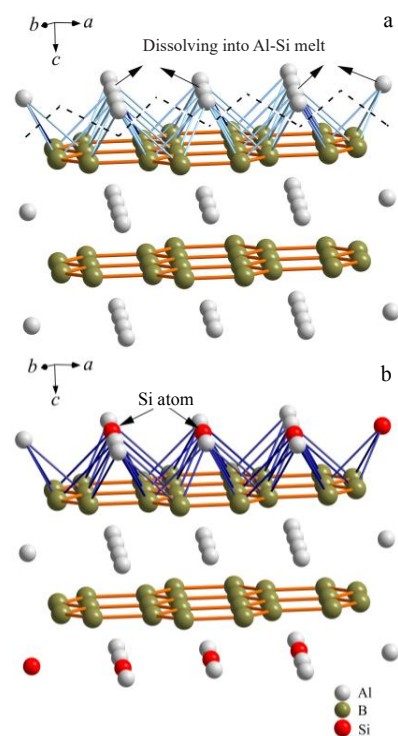


Fig.6 Schematic diagram of the novel atomic model describing the stabilization mechanism of AlB_2 surface and the refining mechanism of α -Al on AlB_2 in Al-Si alloy: (a) Al-Al layer breaking away from the (0001) face of AlB_2 ; (b) formation of new (0001) face with Al-Si atoms in melt and the stabilized outermost surface of AlB_2 for nucleating of α -Al

faster diffusion rate. While, with the existence of AlB_2 as effective nucleant in high Si melt, on the contrary, a few Si atoms are fixed on the surface of AlB_2 and do not form eutectic Si with other Si atoms in the melt. In subsequent cooling stage, because of relatively low diffusion rate, as expected, many Si nanoparticles are precipitated around the surface of AlB_2 particles inside of α -Al^[20]. Combining this experimental result with the atomic mechanism model mentioned above, it is evidently determined that Si atom must be slowly precipitated from the Al-Si two-dimensional atomic layer on the outermost surface of AlB_2 since the solubility of Si in Al-Si atomic layer decreases with declining the temperature, and subsequently nanoscale Si particles neighboring AlB_2 are formed. The forming process of Si nanoparticle is shown in Fig.7.

Based on the above discussion, we have sound reason to infer that Si atoms in Al-Si liquid facilitate the formation and stabilization of AlB_2 particle through firstly inhibiting the nucleation of α -Al to increase undercooling degree of melt; then Al-Si two-dimensional atomic layer grow on AlB_2 surface owing to the decrease of cohesive energy of AlB_2 and the bond energy of Al(Si)-B; finally, Si atoms in two-dimensional Al-Si layer on AlB_2 surface precipitate as nano Si particles at the interface of α -Al/ AlB_2 , which convincingly support the novel

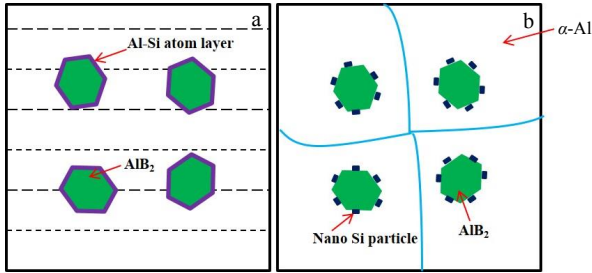


Fig.7 Schematic diagram of forming process of Si nanoparticles:
(a) forming Al-Si layer on AlB₂ surface and (b) participation of Si nanoparticle

refining mechanism of Al-Si alloy proposed in this work.

3 Conclusions

1) The atomic mechanism of heterogeneous nucleation of AlB₂ for α -Al in Al-Si alloy is mainly the formation of Al-Si two-dimensional atomic layer on the outermost surface of AlB₂, which solves the instability problem of Al-Al atomic layer on AlB₂ surface.

2) The cohesive energy of AlB₂ crystal doped with Si decreases with increasing the Si content, which is the key factor leading to the stability of the whole and the outermost surface structure of AlB₂. Simultaneously, the constitutional supercooling caused by Si in Al-Si melt is also an important external factor to promote the formation and stability of the Al-Si two-dimensional atomic layer. Eventually, the strengthening effect of Si atoms on the outermost surface, i.e. Al-Si atomic layer of AlB₂, is the essential reason why AlB₂ can become effective heterogeneous nucleus of α -Al.

References

- Greer L. *J Chem Phys*[J], 2016, 145: 211 704
- Li P, Liu S, Zhang L et al. *Mater Des*[J], 2013, 47: 522
- Nowak M, Bolzoni L, Hari Babu N. *Mater Des*[J], 2015, 66: 366
- Qiu D, Taylor J A, Zhang M X et al. *Acta Mater*[J], 2007, 55: 1447
- Li Y, Hu B, Liu B et al. *Acta Mater*[J], 2020, 187: 51
- Yaguchi K, Tezuka H, Sato T et al. *Mater Sci Forum*[J], 2000, 331-337: 391
- Nafisi S, Ghomashchi R. *Mater Sci Eng A*[J], 2007, 452(24): 445
- Birol Y. *Mater Sci Tech-Lond*[J], 2013, 28(3): 363
- Li J, Yang G, Hage F S et al. *Mater Charact*[J], 2017, 128: 7
- Mohanty P S, Gruzleski J E. *Acta Mater*[J], 1996, 44(9): 3749
- Chen Z N, Wang T M, Gao L et al. *Mater Sci Eng A*[J], 2012, 553: 32
- Sigworth G K, Guzowski M M. *AFS Trans*[J], 1985, 93: 907
- Vinod Kumar G S, Murty B S, Chakraborty M. *Int J Cast Met Res*[J], 2010, 23 (4): 193
- Wang T, Chen Z, Fu H et al. *Met Mater Int*[J], 2013, 19(2): 367
- Kori S A, Murty B S, Chakraborty M. *Mater Sci Eng A*[J], 2000, 283(1-2): 94
- Birol Y. *J Alloys Compd*[J], 2012, 513(3): 150
- Birol Y. *Mater Sci Technol*[J], 2012, 28: 385
- Fan Z, Wang Y, Zhang Y et al. *Acta Mater*[J], 2015, 84: 292
- Han Y F, Dai Y B, Wang J et al. *Appl Surf Sci*[J], 2011, 257: 7831
- Chen Z, Kang H, Fan G et al. *Acta Mater*[J], 2016, 120: 168
- Lin C, Liu Z. *Sci China Ser E*[J], 2008, 51(11): 1867
- Lin C, Zhao Y Q, Yin G L. *Comput Mater Sci*[J], 2015, 97: 86
- Lin C, Yin G L, Zhao Y Q. *Comput Mater Sci*[J], 2015, 101: 168
- Fu B Q, Liu W, Li Z L. *Appl Surf Sci*[J], 2009, 255: 8511
- Fu B Q, Liu W, Li Z L. *Appl Surf Sci*[J], 2009, 255: 9348
- Lin C, Yin G, Zhao Y et al. *Comput Mater Sci*[J], 2016, 111: 41
- Lin C, Huang S, Yin G et al. *Comput Mater Sci*[J], 2016, 123: 263
- Lin C, Yin G L, Zhang A M et al. *Scr Mater*[J], 2016, 117: 28
- Lin C, Liu Z L, Zhao Y Q. *Metall Trans A*[J], 2009, 40(5): 1049
- Lin C, Liu Z L, Zhao Y Q et al. *Mater Chem Phys*[J], 2011, 125: 411
- Lee Y C, Dahle A K, Stjohn D H et al. *Mater Sci Eng A*[J], 1999, 259: 43.
- Maxwell I, Hellawell A. *Acta Mater*[J], 1975, 23: 229
- Zhang H L, Han Y F, Zhou W et al. *Appl Phys Lett*[J], 2015, 106(4): 1
- Fan Z Y. *Mater Trans A*[J], 2013, 44(3): 1409
- Zhang A M, Zhao Z W, Yin G L et al. *Comput Mater Sci*[J], 2017, 140: 61
- Olesinski R W, Abaschian G J. *Alloy Phase Diagrams*[J], 1984, 5: 479

Al-Si合金中 α -Al依附于AlB₂异质形核的原子机制

苏光¹, 张爱民¹, 韦佳宏²

(1. 河南工学院 材料科学与工程学院, 河南 新乡 453000)

(2. 河南工学院 电气工程学院, 河南 新乡 453000)

摘要: 利用固体与分子经验电子理论分别计算了 α -Al, AlB₂与(AI-Si)B₂的价电子结构与结合能。结果表明, AlB₂最外层的Al-Al原子层相对不稳定, 随着Al-Si熔体中Si含量的增加, α -Al和AlB₂的结合能均降低。根据计算结果, 提出了Al-Si合金中 α -Al在AlB₂上异质形核的一种全新原子机制。加入Si后, 一定量的Si原子进入AlB₂, 在AlB₂表面形成稳定的Al-Si二元原子结构层, 提高了AlB₂表面的稳定性。这种稳定的二维Al-Si原子层在随后的异质形核过程中起着重要的过渡作用, 是AlB₂成为 α -Al有效异质核心的原子机制。

关键词: AlB₂晶体结构; Al-Si合金; 异质形核; 原子机制; EET电子理论

作者简介: 苏光, 男, 1977年生, 硕士, 河南工学院材料科学与工程学院, 河南 新乡 453000, E-mail: suguang_hait@163.com